Spallation model coupled with variation of void distribution characteristics and its application*

ZHANG Fengguo*, PAN Hao, WANG Pei, WANG Xinxin

Institute of Applied Physics and Computational Mathematics, Beijing 100094, China

Abstract

At the current stage, the development of spallation damage research is limited because of the lack of real-time experimental methods to capture the variation of void growth and its distribution characteristics, as well as effective mathematical description method to describe the variation of void distribution characteristics. Under strong impact loading, the evolution of spallation damage in ductile materials includes physical processes such as nucleation, growth, coalescence, and final fracture/fragmentation of materials. The growth of voids basically maintains the expansion of spherical holes. The damage evolution process can be divided into two stages: nucleation and growth of voids, and coalescence and growth of voids. The coalescence of voids occurs mainly through direct impingement. Based on the analysis of the variation law of the number of voids in the spallation damage evolution simulated by molecular dynamics, the probability distribution of void nucleation is described using a cosine trigonometric function, and the reduction of void number due to the void coalescence is described using a sine trigonometric function. A phenomenological physical description method for the whole process of the void number density variation is given, and then an evolution equation for spallation damage coupled with the variation law of void number density is constructed. The new model not only fully reflects the physical processes of nucleation, growth and coalescence of voids, but also shows the changing law of void distribution characteristics during damage evolution. The calculation results can determine the damage state and the distribution of void number density in the material, which provides effective support for the analyzing the recompression and fragmentation of materials after spall damage. At the same time, it also promotes the

* The paper is an English translated version of the original Chinese paper published in Acta Physica Sinica. Please cite the paper as: ZHANG Fengguo*, PAN Hao, WANG Pei, WANG Xinxin，**Spallation model coupled with variation of void distribution characteristics and its application**. *Acta Phys. Sin.*, 2026, 75(3):030813. doi: 10.7498/aps.75.20251152

development of spallation damage research. The applicability of the new model is validated by the statistical results of microscopic molecular dynamics computation and related experimental results.

Keywords：spallation model; void nucleation; void coalescence; void distribution characteristics; shock loading; ductile metal

DOI：10.7498/aps.75.20251152

CSTR: 32037.14.aps.75.20251152

1 Introduction

Material deformation and damage failure involve multi-scale cross-level issues ranging from atoms and lattices to grains and macroscopic units. This has long been a significant topic of interest in both the scientific and engineering communities. Effectively diagnosing and accurately describing the multi-scale nonlinear coupling mechanisms between different material levels in experiments, theory, and numerical simulations remains a critical challenge requiring breakthroughs. Spall damage is a primary focus in material damage research due to its theoretical tractability and experimental simplicity. However, spall damage research currently faces bottlenecks because of the lack of experimental methods to capture void growth and distribution changes in real time, as well as the absence of effective mathematical descriptions for these distribution changes [1].

The evolution of spall damage in ductile materials under strong shock loading involves physical processes such as void nucleation, growth, coalescence, and fracture/fragmentation. Void growth generally maintains spherical expansion, and void coalescence occurs primarily through contact [2]. Ideally, the damage evolution process consists of three stages: void nucleation and growth, void growth, and void coalescence and growth [3]. In practice, however, void coalescence may occur prematurely due to the heterogeneous distribution of initial microstructures or local stress concentrations within the material [4]. Therefore, the dynamic tensile damage evolution process is divided into two stages: void nucleation and growth, and void coalescence and growth. To date, research on spall damage has mainly focused on void nucleation [5,6] and growth [7,8], as well as the influence of material microstructures. Examples include the effect of plastic deformation around voids on nucleation [9] and the effect of dislocation evolution on nucleation [10] and growth [11]. Due to theoretical difficulties in analyzing the strong interactions between micro-voids, no robust model currently exists to reasonably describe void coalescence [12]. Existing approaches either describe the effect of void coalescence on damage based on the necking mechanism between two voids of

equal size [13] or use phenomenological methods, such as percolation theory, to analyze the effects of coalescence [14]. These works do not fully reflect the actual physical processes and lack a direct connection to changes in void distribution characteristics during damage evolution. Although one-dimensional calculations can track changes in void number density caused by nucleation and coalescence, this requires tracking void information (size and quantity) for each element at every time step. One-dimensional programs require two-dimensional arrays for data storage, whereas three-dimensional programs for practical engineering applications would require four-dimensional arrays. This results in an enormous data volume that is untenable in engineering practice [3].As refined numerical simulation techniques play an increasingly important role in structural optimization design and the analysis of dynamic material damage mechanisms, This limitation stems from mesh constraints and the incompleteness of existing damage models[15,16]. macroscopic finite element simulations still fail to effectively provide the material damage states and void distribution characteristics required for engineering applications [17]. Consequently, it is necessary to analyze and study the laws governing changes in void distribution characteristics during damage evolution to further develop physical models.

Addressing spall damage in ductile materials under strong shock loading, we aim to seek a phenomenological physical description method for the entire process of void nucleation, growth, coalescence, and changes in void number density. Subsequently, we construct a spall damage evolution equation that couples the laws of void distribution changes. Section 2 briefly introduces the changes in micro-void distribution characteristics during the early stages of void nucleation and growth in spall damage[18]. Thereafter, by analyzing the changes in void distribution characteristics during the later stages of void coalescence and growth, we propose a new spall damage model. We validate the effectiveness and applicability of this model using statistical results from molecular dynamics calculations and relevant experimental data.

2 Physical Description of the Void Nucleation Process

Continuing previous work[18], we select a cosine function form for the void nucleation probability distribution function, namely:

$$g(p) = \frac{1}{p_{\text{spall}} - p_{\text{c0}}}\left[1 - \cos\left(\frac{p - p_{\text{c0}}}{p_{\text{spall}} - p_{\text{c0}}}2\pi\right)\right], \tag{1}$$

In the equation, p denotes the applied tensile stress ($p_{\text{c0}} \leqslant p \leqslant p_{\text{spall}}$) at time t; p_{c0} represents the critical nucleation stress for first void at time t_{c0}, where $p_{\text{c0}} = \frac{2}{3}Y_0[1 +$

$\ln(2G/Y_0)]$ (Y_0 and G denote the yield strength and shear modulus of the material, respectively); p_{spall} indicates the spall strength of the material at time t_{spall}, calculated using a theoretical formula related to the loading strain rate $\dot{\varepsilon}$ proposed by our research group[19],

$$p_{\text{spall}} = \frac{2}{3}Y_0[1 + \ln(2G/Y_0)] + (\frac{Y_0}{GN_0})^{2/9}\rho C_0^{4/3}\dot{\varepsilon}^{2/3}, \quad (2)$$

Here, ρ denotes the material density, N_0 represents the initial microstructural parameter characterizing the influence of grain size and impurity content on void nucleation, and C_0 indicates the bulk wave speed of the material.

To maintain consistency in the theoretical analysis, we continue to employ the void nucleation rate equation proposed by our research group[19]:

$$\dot{N} = N_0 \frac{\dot{p}}{p_{\text{c0}}} \exp(\frac{p - p_{\text{c0}}}{p_{\text{c0}}}). \quad (3)$$

Integrating Equation (3) the number of nucleated voids, N, as

$$N = \int_{p_{\text{c0}}}^{p_{\text{spall}}} \dot{N}\, \mathrm{d}p = N_0[\exp(\frac{p_{\text{spall}} - p_{\text{c0}}}{p_{\text{c0}}}) - 1]. \quad (4)$$

The variation in the cumulative total number of nucleated voids at different time points with increasing stress is

$$N_{\text{t}} = N[\frac{p - p_{\text{c0}}}{p_{\text{spall}} - p_{\text{c0}}} - \frac{1}{2\pi}\sin(2\pi\frac{p - p_{\text{c0}}}{p_{\text{spall}} - p_{\text{c0}}})]. \quad (5)$$

Meanwhile, the evolution equation for the damage variable ϕ (defined as the total void volume per unit volume) is given by

$$\ddot{\phi} = \dot{p}^2(\frac{2\pi}{p_{\text{spall}} - p_{\text{c0}}})^2[K(p - p_{\text{c0}})^{11/2} - \phi], \quad (6)$$

where $K = \frac{8N_0\pi}{33(p_{\text{spall}} - p_{\text{c0}})}(\frac{8}{33\rho\dot{p}^2})^{3/2}$.

Furthermore, the fraction of voids with radii not exceeding a given radius at the cutoff time for void nucleation varies with the void radius as follows:

$$f(a) = (\frac{a}{a_{max}})^{2/3} - \frac{1}{2\pi}\sin[(\frac{a}{a_{max}})^{2/3}2\pi], \quad (7)$$

In the equation, a_{max} denotes the maximum void radius. Figure 1 compares the analytical results from Equation (7) (solid black line) with relevant experimental

data[20]. The two show good agreement, which serves as a primary basis for the subsequent analysis of void coalescence.

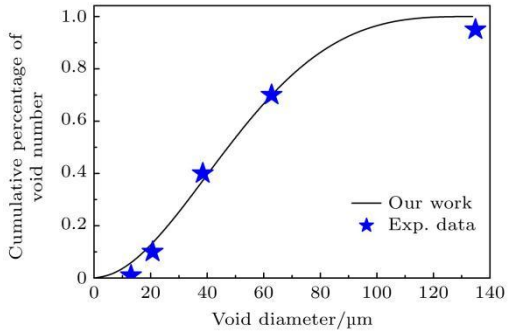

Fig. 1 Cumulative percentage of void count by void size

3 Physical Description of the Void Coalescence Process

3.1 Phenomenological Analysis of the Void Coalescence Process

Under strong shock tensile loading, void coalescence in ductile materials occurs primarily through contact coalescence. This process initiates with the absorption and merging of smaller voids by larger ones. As coalescence progresses, the void number density within the material decreases rapidly. This phenomenon explains why experimental observations during the late stages of damage evolution reveal few voids, which are predominantly large[20]. Furthermore, phenomenological theoretical analysis based on Equation (7) and Figure 1, combined with experimental statistical results, indicates that the void distribution characteristics at the moment between void nucleation cessation and the onset of void coalescence can be approximated by the functional form of Equation (7). In other words, a similar functional form can describe the variation in the proportion of coalesced voids (voids eliminated due to coalescence) relative to the total void count.

3.2 Physical Description of Void Distribution Characteristics During Coalescence

Since material damage is strongly correlated with the total void volume, we first consider two extreme critical cases: 1) At the moment between void nucleation cessation and the onset of void coalescence, the material undergoes complete plastic deformation, and the internal damage degree is $\phi = \phi_0 = Y_0/(2G)$; 2) All voids eventually coalesce into a single void, at which point the internal damage degree is $\phi = \phi_{max} = 1.0$. Thus, the variation in the proportion of voids eliminated due to coalescence relative to the total void count, as damage increases, can be described as

$$W(\phi) = \left(\frac{\phi-\phi_0}{1-\phi_0}\right)^{\frac{2}{3}} - \frac{1}{2\pi}\sin\left[\left(\frac{\phi-\phi_0}{1-\phi_0}\right)^{\frac{2}{3}}2\pi\right]. \quad (8)$$

Clearly, no void coalescence occurs when $W(\phi_0) = 0$. When $W(1.0) = 1$, all voids coalesce to form a single void. However, when $\phi = \phi_{cr} = 0.52$, all voids have come into mutual contact. The damaged material reaches the critical state of network instability. With further development, the material will fracture or fragment, and the damage calculation terminates[2,3].

Therefore, Equations (1) and (8) can comprehensively describe the evolution of void distribution characteristics during the high-dynamic tensile damage process in ductile materials. Given that current experimental techniques lack the capability to statistically monitor changes in internal void number density in real time, we validate the proposed description method using molecular dynamics simulations and metallographic statistical results from spallation experiments. Figures 2 and 3 present the molecular dynamics simulation results[4] and the formula-based calculation results for the temporal evolution of void count at the spallation plane under impact loading velocities of 500 m/s and 750 m/s, respectively. Table 1 lists the loading strain rates, metallographically statistically determined damage degrees, and void number densities at the spallation plane for two pure copper spallation experiments (S24 and S27)[5]. It also includes the void number densities calculated based on Equations (4) and (8) (N_0 = 1.014×10^{15} m^{-3}; see the corresponding literature for material parameters). The comparison indicates that the physical description method for the evolution of void distribution characteristics during spallation damage proposed in this study exhibits good applicability. Furthermore, for different loading strain rate, we determine the corresponding spallation strength using Equation (2). We then calculate the total number of nucleated voids under these strain rate conditions using Equation (4), as shown in Figure 4 (the experimental data in the figure correspond to the total number of nucleated voids for experiments S24 and S27). A higher loading strain rate results in a greater number of nucleated voids, which is qualitatively consistent with observational statistical results from relevant experiments.

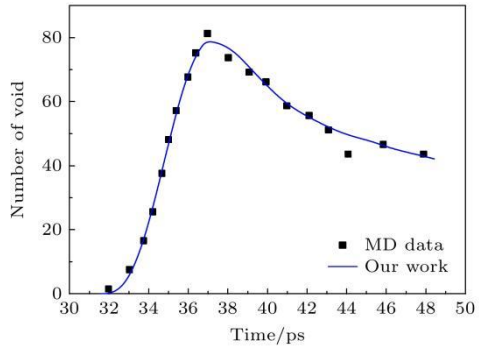

Fig. 2 Variation in void count over time at an impact velocity of 500 m/s within the spall plane.

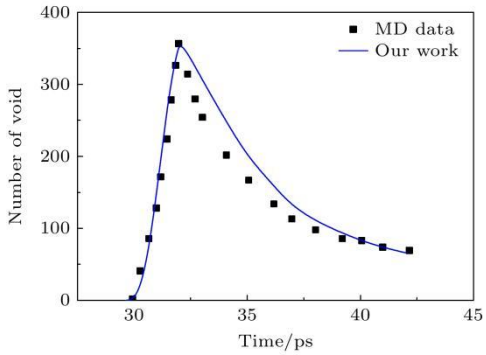

Fig. 3 Variation in void count over time at an impact velocity of 750 m/s within the spall plane.

Table 1 Spall test data.

Experiment No.	Loading strain rate/s-1	Spall strength/GPa	Degree of damage	Void count/(107 cm-3)	
				Experiment	Formula calculation
S24	3.052×104	0.8158	0.277	6.355	6.36
S27	2.321×104	0.8044	0.459	2.16	2.56

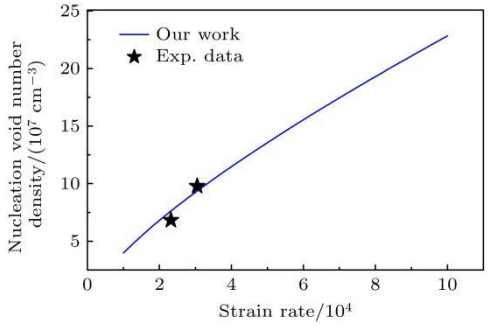

Fig. 4 Nucleation void number density vs. strain rate

3.3 Physical Description of Damage Evolution During Void Coalescence

When the internal damage variable of the material satisfies $\phi \geqslant \phi_0 = Y_0/(2G)$, the material enters a state of fully plastic deformation, and numerous micro-voids form within its interior. Subsequently, the mutual interaction between voids intensifies. It becomes necessary to introduce the porosity parameter $\alpha = 1/(1-\phi)$ and employ a hollow spherical shell cell model to describe void growth. Concurrently, voids of varying sizes begin to coalesce gradually. Therefore, damage growth during this stage involves the combined effects of void growth and void coalescence.

3.3.1 Contribution of Void Growth to Damage Development

Regarding the influence of void growth on damage, we adopt the previously established approach. Based on the relationship between porosity and the damage variable, along with the computational results from the void nucleation and growth stages, when $\phi = \phi_0 = Y_0/(2G)$, according to Equation[3]

$$\frac{1}{2}\tau\frac{\dot{\alpha}^2}{(\alpha-1)^{4/3}} = \alpha p(t) - \frac{2}{3}Y_T \ln\left(\frac{\alpha}{\alpha-1}\right) \tag{9}$$

Determine the model parameter τ. Subsequently, employ the unit cell model proposed by Johnson[7] to describe void growth:

$$\begin{aligned}\tau\{\ddot{\alpha}[(\alpha-1)^{-\frac{1}{3}} - \alpha^{-\frac{1}{3}}] - \frac{\dot{\alpha}^2}{6}[(\alpha-1)^{-\frac{4}{3}} - \alpha^{-\frac{4}{3}}]\} \\ = \alpha p(t) - \frac{2}{3}Y_0 \ln\left(\frac{\alpha}{\alpha-1}\right).\end{aligned} \tag{10}$$

3.3.2 Contribution of Void Coalescence to Damage Evolution

As previously discussed, under high-intensity shock loading, voids within damaged materials primarily coalesce through contact. The influence of void coalescence on porosity growth is described as[2]

$$\dot{\overline{\alpha}} = \dot{\alpha}\sqrt{\frac{\sum(n_i/r_i)}{\sum(N_j/R_j)}}, \tag{11}$$

Here, $\dot{\alpha}$, r_i, and n_i denote the porosity growth rate, void radius, and corresponding void number density before void coalescence, respectively; $\dot{\overline{\alpha}}$, R_j, and N_j represent the corresponding parameters after void coalescence. Equation (11) requires tracking the growth evolution of all voids and changes in their respective counts. This approach incurs substantial computational and storage costs in practical three-dimensional engineering simulations. To address this, we employ a

phenomenological averaging method. By considering the conservation of total void volume before and after contact coalescence, we derive the following analogous formulation:

$$\dot{\overline{\alpha}} = \dot{\alpha}\sqrt{\frac{\sum(n_i/r_i)}{\sum(N_j/R_j)}} \approx \dot{\alpha}\sqrt{\frac{\sum(n/r)}{\sum(\overline{N}/R)}} = \dot{\alpha}\frac{n^{2/3}}{\overline{N}^{2/3}}, \tag{12}$$

In the equation, r and n denote the average void radius and void number density before void coalescence, respectively; R and $\overline{N}$ represent the average void radius and void number density after void coalescence, respectively. Furthermore, in conjunction with Eq. (8), the contribution of void coalescence to the development of spall damage can be expressed as

$$\begin{aligned}\left(\frac{\dot{\overline{\alpha}}}{\dot{\alpha}}\right)^{3/2} &= \frac{n}{\overline{N}} = \frac{N(1-W(\varphi))}{N[1-W(\varphi+\Delta\varphi)]} \\ &= \frac{1-W(\varphi)}{1-W(\varphi+\Delta\varphi)}.\end{aligned} \tag{13}$$

4 Application and Analysis of the New Spall Damage Model

The primary procedure for damage calculation is as follows: When the tensile stress within an element exceeds the critical void nucleation stress p_{c0}, the spall strength p_{spall} and the total number of nucleated voids N are first calculated based on the strain rate of that element using Equations (2) and (4). Subsequently, the number of voids and the evolution of damage during the stages of void nucleation and growth are determined using Equations (5) and (6). When $\phi = \phi_0 = Y_0/(2G)$, the model parameter τ is determined based on the current stress and damage state of the element using Equation (9). Finally, when $\phi \geqslant Y_0/(2G)$, the number of voids and damage evolution during the stages of void coalescence and growth are calculated using Equations (8) and (10). The influence of void coalescence on damage growth is then computed using Equation (13).

The S24 experiment involved a 0.62 mm thick pure copper flyer plate impacting a 1.59 mm thick pure copper target plate at a velocity of 159 m/s. A PMMA backing plate was attached to the rear of the target to measure the history of stress changes. The material parameters and damage model parameters provided in the corresponding literature were adopted. Figures 5 and 6 present the damage distribution and void number density distribution within the target plate, respectively. These figures include the calculation results from this study, as well as the results from the NAG model (nucleation and growth model) and experimental data reported in the literature[5]. The results indicate that the calculations from this study align better with the experimental

data than those from the NAG model. This improvement is attributed to the inclusion of void coalescence calculations in the present model, the void number density distribution of the central region is slightly lower than the experimental values. The higher values on both sides compared to the experiment may be due to the exclusion of smaller micro-voids in the experimental statistical analysis.

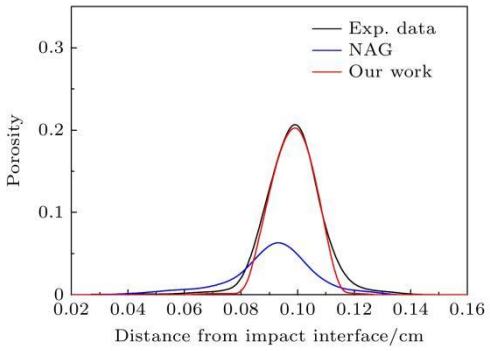

Fig. 5 Computed and observed damage in the copper target.

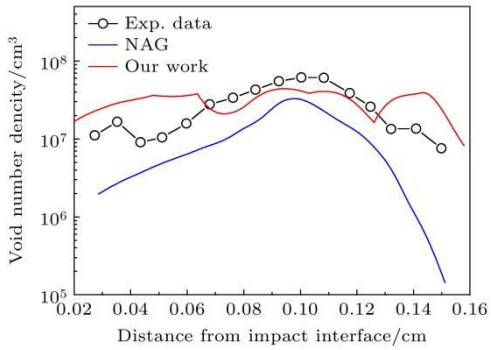

Fig. 6 Computed and observed void concentrations in the copper target.

Furthermore, this study compares our spall damage calculation method with the widely used VG model[7] (void growth model) and the NAG model[5]. The evolution of damage at the spall plane is further analyzed. The VG model involves three parameters: initial porosity, a viscosity coefficient, and a hardening coefficient, all related to the material's physical properties. The NAG model includes six parameters: the coefficient N_0 related to the initial microstructure, the initial nucleation void radius, a viscosity coefficient, the critical stress for void nucleation, the critical stress for void growth, and a reference stress. In contrast, the proposed spall damage calculation method requires only one parameter, N_0, which relates to the initial microstructure but remains independent of the material's physical properties. This independence constitutes a significant advantage. Damage evolution processes calculated by different models vary significantly. In numerical simulations, damage calculation couples with constitutive and equation-of-state computations. Consequently, spall plane positions may differ slightly across models. Therefore, comparing damage evolution in elements at identical

positions or those experiencing maximum damage may be inappropriate. To address this, the numerical calculation considers damage evolution only for elements at the same spall plane position. Damage is not calculated for any other elements. Figure 7 compares the experimental free-surface velocity measurements[21] for a 2 mm pure copper flyer impacting a 9 mm pure copper target at 185 m/s with the results from the three spall damage models. As shown in Figure 7, the results from the three models are similar. Compared with the experimental data, all computational results capture the rebound point of the velocity curve and the subsequent oscillation period characteristics. Figure 8 shows the damage evolution histories calculated by the three models for elements at the spall plane. The new model exhibits the fastest damage development because it accounts for void coalescence. The NAG model employs the void growth equation for an infinite medium, a strong constraint, and ignores void coalescence. Both Figure 5 and Figure 8 show that the damage calculated by the NAG model is significantly lower than that from other models and experimental statistics. Additionally, experimental results by Rivas et al.[20] indicate that damage levels within materials can differ by orders of magnitude even when free-surface velocities are similar. This suggests that calibrating damage models solely using simulated free-surface velocities is incomplete. Figure 9 illustrates the variation in void number density within the element. The new model demonstrates the physical process where the void count rapidly increases due to void continuous nucleation and gradually decreases due to void continuous coalescence. In contrast, the NAG model calculates only void growth, which deviates significantly from the actual physical process.

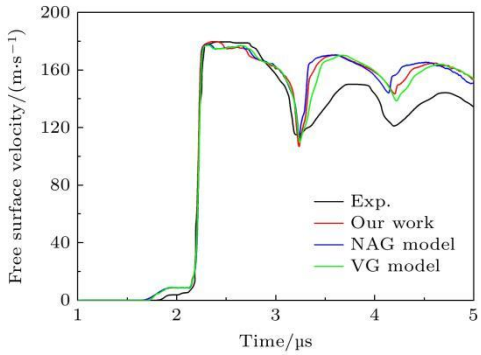

Fig. 7 Experimental and computed free-surface velocity profiles using VG, NAG, and our model.

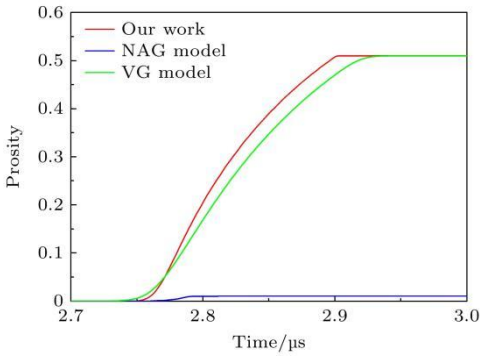

Fig. 8 Computed damage evolution using VG, NAG, and our model.

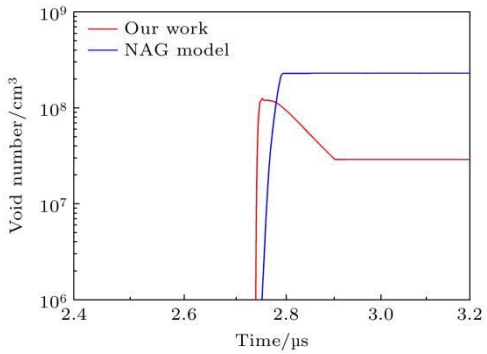

Fig. 9 Computed void number using NAG and our model.

Thus, by employing Equations (1) and (8), we achieve a phenomenological description of the evolving microvoid distribution characteristics during spall damage evolution. This approach avoids the need to track and record the size and quantity of voids in each element at every time step during numerical calculations. Consequently, it facilitates two-dimensional and three-dimensional numerical simulations and allows for the quantitative determination of the material spall damage state. Furthermore, addressing the issue of micro-spallation, we incorporate the correlation between the final damage state-specifically void distribution characteristics and material fragmentation granularity-along with the effects of ambient temperature and temperature rise induced by material deformation. Drawing on our previously established methodology[3], we achieve a physical description of the entire process from void nucleation to material fragmentation.

5 Conclusions

This study introduces a trigonometric probability distribution function to describe void nucleation and coalescence. This approach successfully decouples the interdependence between damage and void distribution. It not only provides a comprehensive description of the evolution of void distribution characteristics during spall damage but also establishes a new spall damage model that couples changes of the

internal microstructural information in the material. Moreover, this model can be effectively applied to simulate and analyze two-dimensional and three-dimensional spall damage problems in practical engineering structures. The new damage model currently contains only one parameter related to the initial microstructure of the material, independent of its physical and mechanical properties. Compared to other damage models with multiple parameters, this model may offer better applicability. Additionally, calculations using the new damage model can determine the material damage state and the internal void distribution characteristics. These capabilities provide effective data support for investigating issues such as the recompression of damaged materials and the particle size distribution resulting from damage-induced fragmentation.

However, although we validated the applicability of the new model using molecular dynamics statistical results and experimental data from two data points, the limited number of experimental points and their similar loading strain rate ranges constrain the validation. Given that current experimental techniques cannot provide real-time data on the change of void distribution characteristics during damage evolution, further validation of the new model's applicability and scope requires experimental data across a broader range of loading strain rates. Such data should include free surface velocity, the damage state within recovered target plates, and void distribution characteristics.

References

[1] Dongare A M 2020 *J Mater Sci* **55** 3157

[2] Zhang F G, Zhou H Q, Hu X M, Wang P, Shao J L, Feng Q J 2016 *Explo. Shock Waves* **36** 596

[3] Zhang F G, Liu J, He A M, Zhao F Q, Wang P 2022 *Acta Phys. Sin.* **71** 244601

[4] Dongare A M, Rajendran A M, LaMattina B, Zikry M A, Donald W, Brenner D W 2010 *J. App. Phys.* **108** 113518

[5] Seaman L, Curran D R, Shockey D A 1976 *J. App. Phys.* **47** 4814

[6] Molinari A, Wright W A 2005 *J. Mech. Phys. Solids* **53** 1476.

[7] Johnson J N 1981 *J. App. Phys.* **52** 2812

[8] Gurson A L 1977 *J. Eng. Mater. Technol.* **99** 2

[9] Trumel H, Hild F, Roy G, Pellegrini Y P, Denoual C 2009 *J. Mech. Phys. Solids* **57** 1980

[10] Sui H N, Yu L, Liu W B, Liu Y, Duan H L 2022 *J. Mech. Phys. Solids* **168** 105032

[11] Wilkerson J W 2017 *I. J. Plasticity* **95** 21

[12] Huang Z P, Yang L M, Pan K L 1993 *Adv. Mech.* **23** 433

[13] Tonks D L, Zurek A K, Thissell W R 2003 *J. Phys. IV* **110** 893

[14] Wang Y G, He H L, Wang L L, Jing F Q 2006 *Chin. J. High Pressure Phys.* **20** 127

[15] Chen X, Asay J R, Dwivedi S K, Field D P 2006 *J. Appl. Phys.* **99** 023528

[16] Lescoute E, De Rességuier T, Chevalier J M, Loison D, Cuq-Lelandais J P, Boustie M, Breil J, Maire P H, Schurtz G 2010 *J. Appl. Phys.* **108** 093510

[17] Liu J, Sun Z Y, Zhang F G, Wang P 2022 *Explo. Shock Waves* **42** 033101

[18] Zhang F G, Wang Y J, Wang P, Wang X X 2025 *Acta Phys. Sin.* **74** 014601

[19] Zhang F G, Zhao F Q, Liu J, He A M, Wang P 2022 *Acta Phys Sin.* **71** 034601

[20] Rivas J M, Zurek A K, Thissell W R, Tonks D L, Hixson R S 2000 *Metall. Mater. Trans. A* **31** 845

[21] Rajendran A M, Dietenberger M A 1989 *J. Appl. Phys.* **65** 1521